



# Numerical analysis on stability of nuclear fuel plates with inlet support comb



Javier González Mantecón\*, Miguel Mattar Neto

Instituto de Pesquisas Energéticas e Nucleares, IPEN-CNEN/SP, Av. Prof. Lineu Prestes, 2242 – Cidade Universitária, CEP 05508-000 São Paulo, SP, Brazil

## ARTICLE INFO

### Keywords:

Plate-type fuel element  
Support comb  
Fluid-structure interaction  
Critical velocity

## ABSTRACT

Many nuclear research reactors use or are planned with cores containing flat-plate-type fuel elements. One of the problems of this fuel element design is the mechanical stability of the fuel plates. High-velocity coolant flowing through the narrow channels that separate the plates can cause large deflections of these plates leading to local overheating, structural failure or plate collapse. In particular, in real fuel elements and experimental tests, flow-induced deflections at the leading edge and along the length of the plates have been detected. Some authors have indicated that the use of a support comb removes the leading-edge static divergence, but it has been also suggested that, even with the comb, there are significant deflections away from the inlet.

In this work, a fluid-structure interaction study is conducted to examine the effectiveness of using an inlet comb on the mechanical stability of fuel plates. The system consists of two fuel plates bounded by three-equal coolant channels. The pressure loadings caused by the fluid flow are calculated using a CFD model and the structural response of the plates and the support comb are determined by means of an FEA model. The two-way fluid-structure interaction method was employed for coupling the fluid and solid solvers.

The results presented here show that the static divergence at the inlet end is effectively eliminated with the installation of a support comb. Nevertheless, the main contribution of this work is the detection of deformation of the plates along their length and that it was an increasing function of the fluid velocity in the channels. As a consequence, the flow channels could be constricted or completely closed, thus affecting the safe operation of the nuclear reactor. To the best of our knowledge, this is the first numerical analysis reported in the literature that models the fluid-structure interaction phenomenon of adjacent plates with the support comb located at the midpoint of their inlet end.

## 1. Introduction

Many nuclear research reactors use or are planned with cores containing flat-plate-type fuel elements. One of the problems of this fuel element design is the mechanical stability of the fuel plates. High-velocity coolant flowing through the narrow channels that separate the plates has the potential to cause deflections of these plates. First noticed by Stromquist and Sisman (1948), this phenomenon has been of concern to engineers because large deflections may cause local overheating and probably a whole blockage of the channels.

Daniel Miller reported that there is a “critical velocity” above which structural failure or plate collapse would occur in a flat-plate-type fuel assembly (Miller, 1958). Miller determined this velocity based on the interaction between the changes in cross-sectional areas, coolant velocities and pressures in two neighboring coolant channels. For a multiple plate assembly with fixed edges, the Miller’s critical velocity is defined

as:

$$v_M = \left[ \frac{15Ea^3h}{\rho w^4(1-\nu^2)} \right]^{1/2} \quad (1)$$

where  $E$  is the Young’s Modulus of elasticity,  $a$  the fuel plate thickness,  $h$  the coolant channel thickness,  $\rho$  the density of the coolant,  $w$  the wetted plate width (channel width) and  $\nu$  the Poisson’s ratio.

In experimental setups, flow-induced deflections at the inlet end and along the length of the plates have been identified (Groninger and Kane, 1963; Ho et al., 2004; Kennedy, 2015; Smislaert, 1968). Deflections were detected at coolant velocities below the critical velocity. In those previous works, the leading edge of the fuel plates was identified as the most susceptible portion. Smislaert named the deflection at the inlet end as *static divergence* (Smislaert, 1968).

Some authors have indicated that the use of an inlet support comb removes the leading-edge static divergence (Groninger and Kane, 1963;

\* Corresponding author.

E-mail address: [javier.mantecon@ipen.br](mailto:javier.mantecon@ipen.br) (J. González Mantecón).

<https://doi.org/10.1016/j.nucengdes.2018.12.009>

Received 17 September 2018; Received in revised form 27 November 2018; Accepted 10 December 2018

Available online 19 December 2018

0029-5493/ © 2018 Elsevier B.V. All rights reserved.

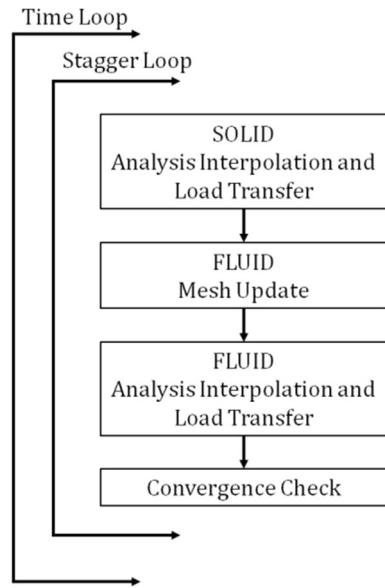


Fig. 1. Levels of iterations of a transient two-way FSI analysis [modified from (Rao, 2003)].

Johansson, 1959; Smitsaert, 1969, 1968). Nevertheless, according to Groninger and Kane (1963), even with a comb “there are significant deflections two or three plate spans away from the inlet to the sub-assembly”. Since Smitsaert (1969), almost no investigations have been concerned with the analysis of nuclear fuel plates with the inlet comb. After a thorough review of the available literature, we can only mention a technical report with a direct relationship to the topic being discussed (Tentner et al., 2017). In that study, a numerical analysis was completed using the Abaqus software. It was applied a rigid mechanical stop that prevented the deflection of the plate at its leading edge and was found that the maximum deflection occurred near the outlet end. It was recommended to run additional simulations for understanding how the maximum deflection and its location change when the comb is used. One of the limitations of that work is that only one plate was simulated. According to Smitsaert (1969), the lift force acting on one leading edge is affected by the existence of adjacent plates. Therefore, an analysis that considers that effect is desired.

In view of the very limited number of works that investigate the influence of the inlet support comb, the authors conducted numerical tests to examine the effectiveness of using this device on the mechanical stability of fuel plates. For this purpose, a non-linear fluid-structure interaction (FSI) model by coupling the Computational Fluid Dynamics (CFD) code ANSYS CFX and the Finite Element Analysis (FEA) code ANSYS Mechanical was developed (ANSYS Inc., 2017a,b). The fluid-

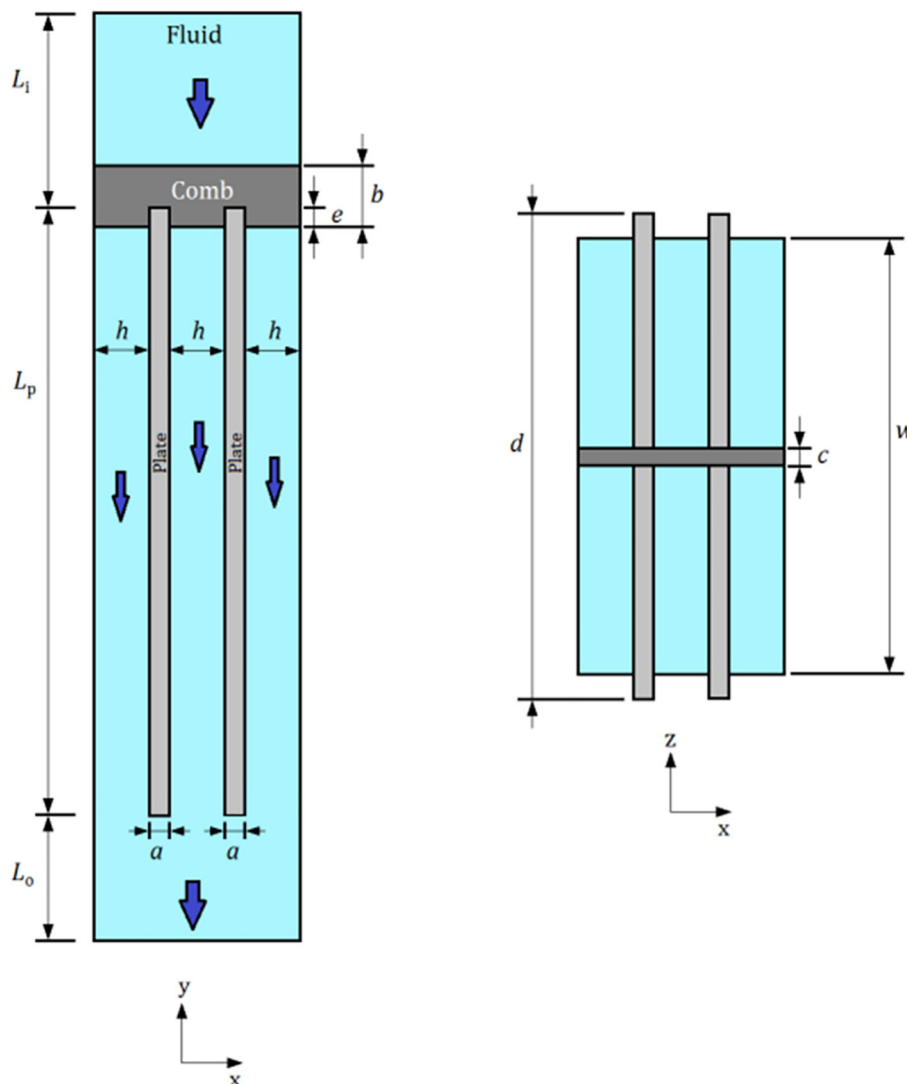


Fig. 2. Illustration of the computational domain: longitudinal view (left) and top view (right).

**Table 1**  
Geometric characteristics of the domain.

Parameter	Symbol (unit)	Value
Channels – thickness	$h$ (mm)	2.45
Channels – width	$w$ (mm)	70.5
Channels (plates) – length	$L_p$ (mm)	655
Plates – thickness	$a$ (mm)	1.35
Plates – width	$d$ (mm)	75
Inlet plenum – length	$L_i$ (mm)	190
Outlet plenum – length	$L_o$ (mm)	70
Support comb – height	$b$ (mm)	40
Support comb – thickness	$c$ (mm)	8
Support comb – finger	$e$ (mm)	11.5

solid computational domain consists of two-equal plates with an inlet comb and bounded by three-equal coolant channels. The pressure loadings caused by the fluid flow were calculated using the CFD model and the structural response was determined by the FEA model. The two-way fluid-structure interaction method was employed for coupling the fluid and solid solver. To the best of our knowledge, this is the first numerical analysis reported in the literature that models FSI phenomenon of adjacent plates with the support comb located at the midpoint of their inlet end.

**2. Multiphysics analysis**

In fluid-structure interaction simulations, the fields are interfaced via the so-called wet surface where the pressure and friction forces produced by the fluid are acting on the structure. Because of the pressure loads caused by the flow, the body becomes deformed changing the boundaries of the fluid domain and, as a result, the flow pattern.

In this study, in order to solve the multiphysics problem, two codes were utilized: one code solved the fluid dynamics (ANSYS CFX) and the other one the structural part of the domain (ANSYS Mechanical – Transient Structural). Both solvers were coupled using the two-way coupling method (ANSYS Inc., 2017a). During FSI calculations, the solvers calculate the solution considering one (*explicit*) or many (*implicit*) coupling iterations, and the information is exchanged between them. The process of data sharing continues until the required

**Table 2**  
Mesh characteristics for verification of the CFD model.

Mesh	Domain Volume (mm <sup>3</sup> )	Number of Elements	Refinement Factor, $r$	$P_{max}$ (Pa)
1	520,650	1,035,584	1.125	135,444
2		729,312	1.243	135,323
3		379,269	–	135,479

**Table 3**  
Uncertainty quantification of the CFD model.

Parameter	Value
$\varphi_{ext}^{21}$	136086.48 Pa
$e_a^{21}$	0.09%
$GCI_{21}$	0.59%

**Table 4**  
Mesh characteristics for verification of the structural model.

Mesh	Domain Volume (mm <sup>3</sup> )	Number of Elements	Refinement Factor, $r$	$\delta_m$ (mm)
1	135,605	299,656	1.249	0.5110
2		153,942	1.246	0.5104
3		79,428	–	0.5095

**Table 5**  
Uncertainty quantification of the structural model.

Parameter	Value
$\varphi_{ext}^{21}$	0.5121 mm
$e_a^{21}$	0.11%
$GCI_{21}$	0.27%

conditions are satisfied.

In an implicit two-way coupling simulation, data between the solvers is exchanged many times in a time step and until the convergence is reached. Afterward, a new time step begins. The drawback of this

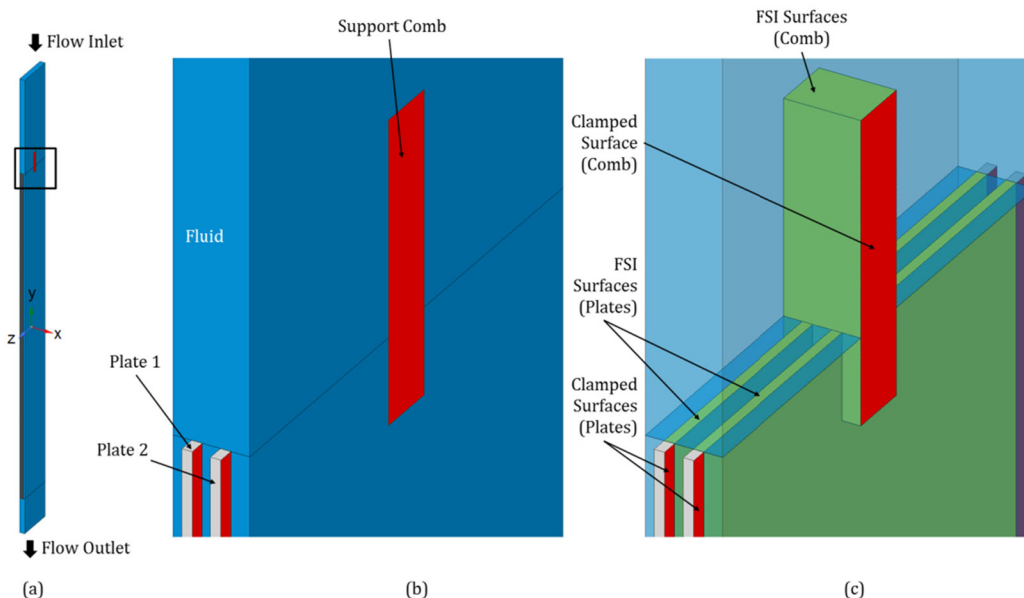


**Fig. 3.** Multiphysics domain. (a) Full view, (b) and (c) close view at the leading edge. The red surfaces identified the clamped regions; the green surfaces are the FSI regions. (For interpretation of the references to colour in this figure legend, the reader is referred to the web version of this article.)

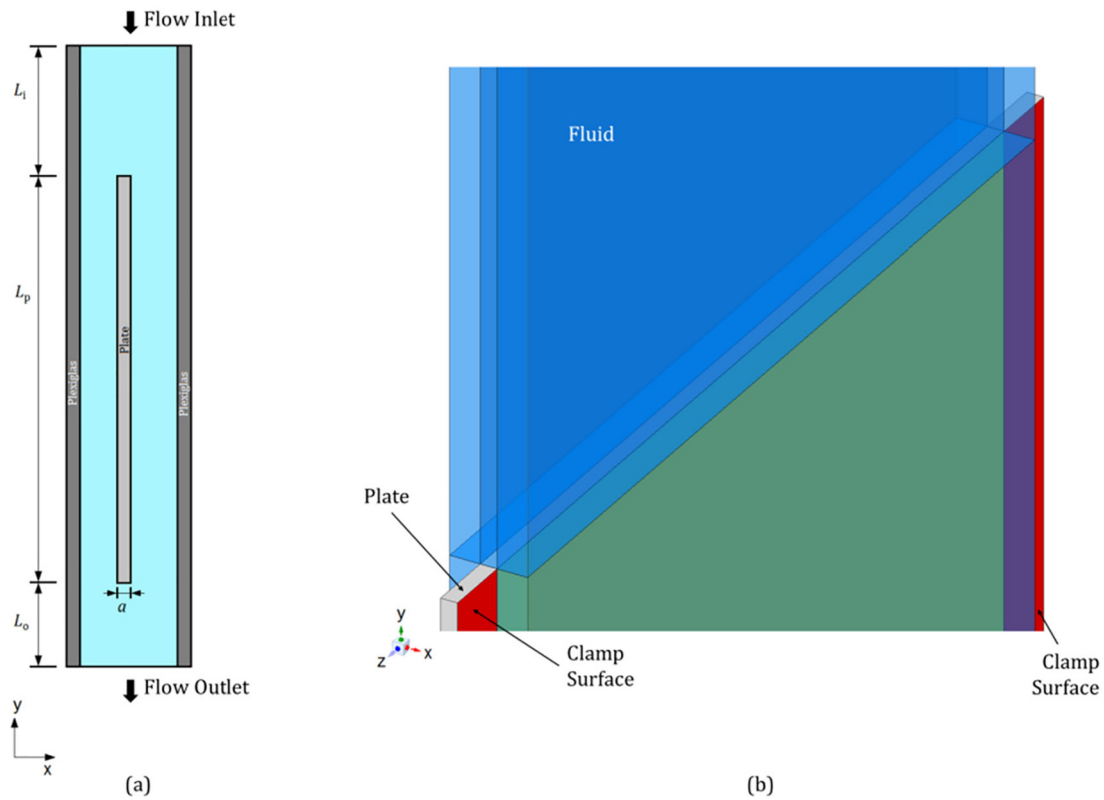


Fig. 4. (a) Schematic representation of Kennedy's one-plate experiment and (b) FSI model.

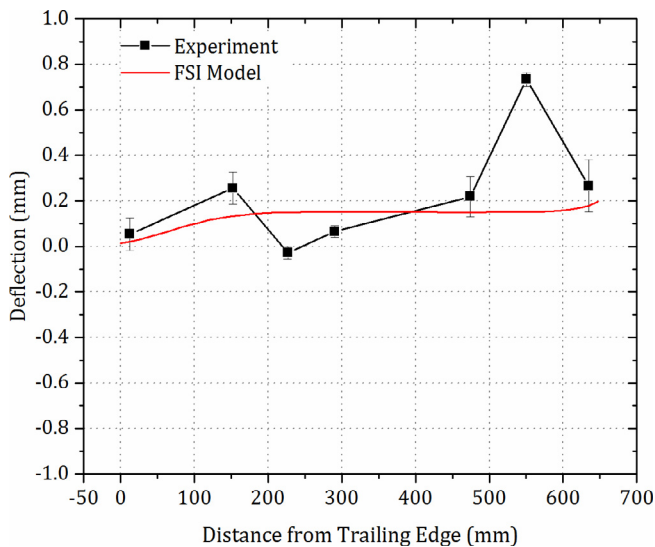


Fig. 5. Comparison of the plate deflections with the experiment.

Table 6  
Volume flow rates and fluid velocities used in this work.

Simulation	$Q_{in}(m^3/h)$	$v_{in}(m/s)$	$Re_{in}$
1	15.30	6.00	118,696
2	18.85	7.39	146,194
3	21.99	8.62	170,527
4	25.12	9.85	194,860
5	28.26	11.09	219,391
6	31.42	12.32	243,723
7	34.56	13.55	268,056
8	37.70	14.78	292,389

technique is that there is a considerable increment of computational cost. In contrast, in explicit two-way coupling simulations, smaller time steps are required; the convergence at the fluid-solid interface during a time step may be not considered and a new time step is launched directly. However, at the end of the simulation time, the convergence is necessary. Taking into consideration the available computational resources and that we are interested in the steady-state and static deflection of the plates, we chose the explicit scheme. Fig. 1 shows the process flowchart for the two-way coupling algorithm.

### 3. Numerical methodology

The multiphysics model was created with hydraulic and geometric characteristics of a typical fuel element of the upcoming Brazilian Multipurpose Reactor (RMB - acronym in Portuguese) (Perrotta and Soares, 2015). Each RMB's fuel element has 21 plates with a meat made of low enriched Uranium Silicide-Aluminum dispersion ( $U_3Si_2-Al$ ) clad with Aluminum. The dimensions of the assembly are  $80.5\text{ mm} \times 80.5\text{ mm} \times 1045\text{ mm}$ . A generic diagram of the studied domain is shown in Fig. 2 and Table 1 details its geometric specifications. In that figure, the fluid flow direction is indicated by the dark blue arrows.

#### 3.1. Fluid model

The fluid domain was modeled using ANSYS CFX. It was composed of an inlet plenum, coolant channels, and an outlet plenum (see Fig. 2) and was divided into different volumes to create a hexahedral mesh. A mesh sensitivity study according to ASME V&V 20-2009 best practice guidelines (ASME, 2009) for the estimation of uncertainty because of the spatial grid was performed and it is described further in this paper. In Fig. 3 the multiphysics domain is shown. Fig. 3(c) depicts a transparent view of the domain where it is possible to observe the surfaces of the solid part in contact with the fluid flow.

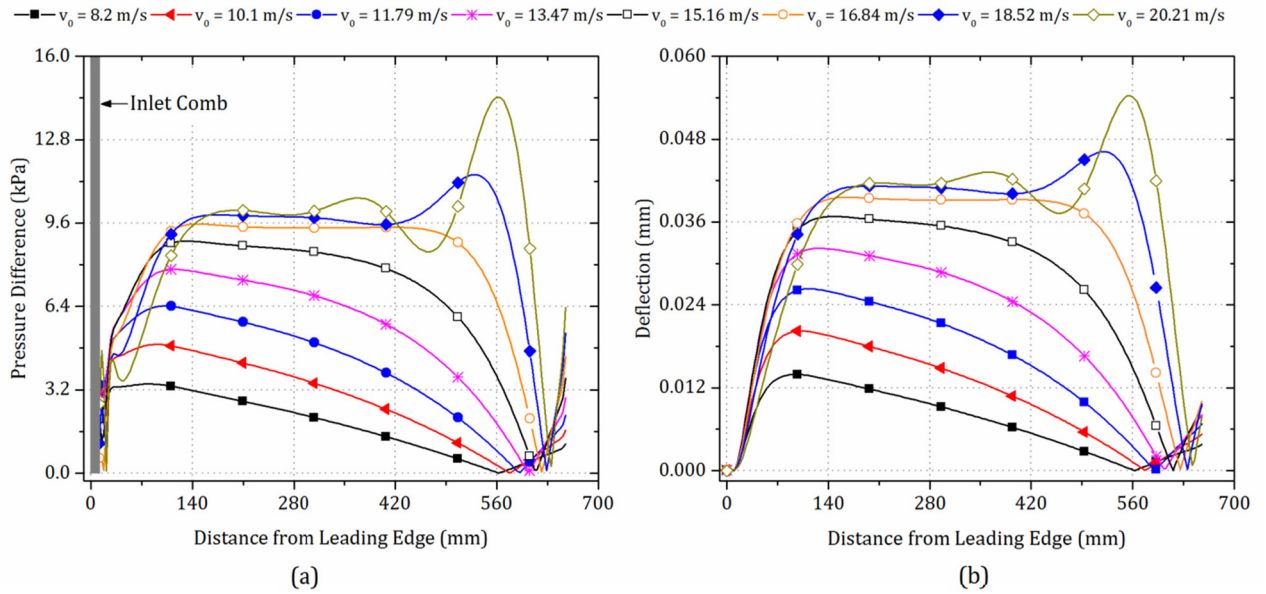


Fig. 6. The pressure difference across Plate 2 and deflection profile of Plate 2 for different coolant velocities in the channels, with the support comb at the inlet end of the plates.

The fluid around the plates is water at room temperature with constant physical properties: density of  $997.56 \text{ kg/m}^3$  and dynamic viscosity ( $\mu$ ) of  $8.87 \times 10^{-4} \text{ Pa}\cdot\text{s}$ . At the inlet of the CFD domain, a uniform fluid velocity ( $v_{in}$ ) was assumed and was defined by the following expression:

$$v_{in} = \frac{3h}{3h + 2a} v_0 \quad (2)$$

In the above equation,  $v_0$  is the average water velocity in the coolant channels. Coolant velocities at the inlet of the domain along with the Reynolds numbers are provided later in this paper. At the outlet, the zero-gauge pressure condition was set.

The fluid surfaces in contact with the plates were assumed deformable, no-slip walls, with a roughness height (arithmetic average) of  $0.1 \mu\text{m}$  and equivalent sand-grain roughness height of  $0.5863 \mu\text{m}$  (Adams et al., 2012; ANSYS Inc., 2017a). The same sand grain roughness was considered at the no-slip rigid walls parallel to the plates and in the flow direction; this condition is used to simulate the surfaces of neighboring plates enclosing the external coolant channels. The fluid surfaces in contact with the support comb were also considered as no-slip deformable walls and were treated as smooth surfaces. The no-slip wall boundary condition was imposed at the outer surfaces of the domain and they were treated as smooth surfaces, except those modeling adjacent plates.

To numerically solve the unsteady turbulent flow, the standard  $k-\epsilon$  turbulence model with scalable wall functions was adopted. This turbulence model is widely used in handling many turbulent fluid engineering problems, and it has proven to be numerically robust, stable and with well-established predictive capabilities on problems involving narrow channels of nuclear research reactors (de Andrade et al., 2015; Fan et al., 2015). In all simulations, the energy equation was neglected; double precision and a time step of  $0.025 \text{ s}$  were utilized. Finally, a root mean square (RMS) residual target of  $10^{-4}$  as the convergence criterion and a minimum of two iterations per time step were considered.

### 3.1.1. Fluid model verification

A solution verification study was conducted according to the ASME guidelines (ASME, 2009) to assess the numerical accuracy and to determine the adequacy of the CFD mesh for the FSI simulations. The Grid Convergence Index (GCI) was employed for estimation and reporting of uncertainty due to discretization. The theoretical basis of the method is

to assume that solutions converge asymptotically towards the exact solution as the number of elements is incremented with an apparent order of convergence that is theoretically proportional to the order of discretization scheme. The aim of the method is to estimate a 95% confidence interval that contains the exact solution.

For this mesh study, steady-state analyses with three progressively refined structured hexahedral meshes were completed. In this specific case, all fluid surfaces in contact with the solid material were considered as rigid walls and, by using Eq. (2), an inflow velocity of  $6.0 \text{ m/s}$  was set. This velocity was determined considering an average fluid velocity in the channels of  $8.2 \text{ m/s}$ , which is the minimum velocity required in an RMB's fuel assembly (INVAP, 2013). The other conditions are the same as previously mentioned. The GCI for the finest mesh was calculated by using Eqs. (3)–(8); the maximum pressure ( $P_{max}$ ) on the surfaces of the plates was selected as the key parameter. Details of the meshes are presented in Table 2, where the finest mesh is designated as Mesh 1.

$$GCI_{21} = \frac{1.25e_a^{21}}{r_{21}^p - 1} \quad (3)$$

$$p = \left[ \frac{1}{\ln(r_{21})} \right] \left[ \ln \left| \frac{\varphi_3 - \varphi_2}{\varphi_2 - \varphi_1} \right| + q(p) \right] \quad (4)$$

$$q(p) = \ln \left( \frac{r_{21}^p - s}{r_{32}^p - s} \right) \quad (5)$$

$$s = 1 \cdot \text{sign} \left( \frac{\varphi_3 - \varphi_2}{\varphi_2 - \varphi_1} \right) \quad (6)$$

$$\varphi_{ext}^{21} = \frac{r_{21}^p \varphi_1 - \varphi_2}{r_{21}^p - 1} \quad (7)$$

$$e_a^{21} = \left| \frac{\varphi_1 - \varphi_2}{\varphi_1} \right| \quad (8)$$

In the above equations,  $p$  is the apparent order of convergence and it is calculated with an iterative procedure,  $r$  is the refinement factor,  $\varphi$  is the variable of interest found with gradually refined mesh,  $\varphi_{ext}^{21}$  is the extrapolated value of the variable of interest and  $e_a^{21}$  is the approximate relative error.

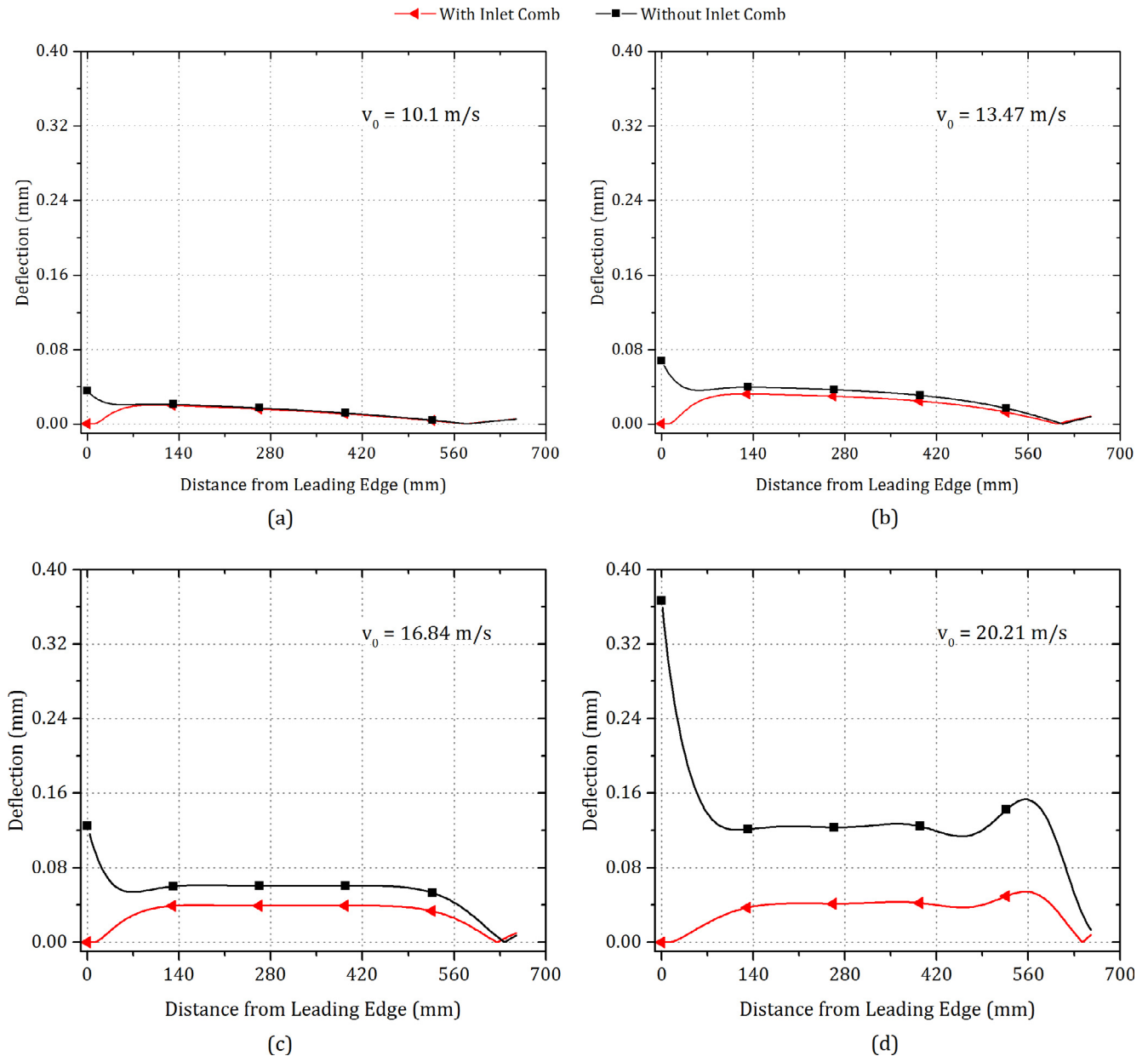


Fig. 7. Deflection profile along the centerline of Plate 2 for different coolant velocities in the channels, with and without the support comb at the inlet end of the plates.

Table 3 presents the results obtained with the ASME standard. The three meshes showed a well behaved convergence and the predicted uncertainty can be considered as a reliable approximation of the correct solution. Therefore, the authors consider that, for the FSI analysis, a mesh with 1,035,584 elements is sufficient as the numerical uncertainty for the maximum pressure on the surfaces of the plates was 0.59%.

### 3.2. Structural model

In the fuel plates here studied, the fuel meat consists of a fuel powder dispersed in an Aluminium matrix and clad with this same material. Hence, the plate material considered is Aluminium Alloy 6061-T6. The material of the comb was assumed to be the same. The properties of the Al-6061-T6 at room temperature are: Poisson’s ratio of 0.33, Young’s Modulus of 68.9 GPa, density ( $\rho_s$ ) of 2700 kg/m<sup>3</sup> and yield strength ( $\sigma_y$ ) of 276 MPa (ASM International, 1990). The plasticity material model (Bilinear Isotropic Hardening) with zero Tangent Modulus was considered.

The structural part of the multiphysics domain was modeled using the Transient Structural module of ANSYS Mechanical. The plates and the inlet support comb were discretized using a structured mesh with SOLID186 hexahedral elements (ANSYS Inc., 2017b). Along the sides parallel to flow, a 2.25 mm region of the width of each plate was used to clamp them. The boundary condition on front and back faces were displacements in  $x = y = z = 0$ . The surfaces of the support comb and plates that are in contact were modeled as Frictionless Contacts and CONTA174 elements were utilized. This element type is used to represent contact and sliding between 3-D target surfaces and a deformable surface (ANSYS Inc., 2017b). A Fluid-Solid Interface boundary condition was assumed on the surfaces of the comb and plates in contact with the fluid. These are the surfaces where pressure loads from the CFD model are applied. The trailing edge of each plate was free.

#### 3.2.1. Structural model verification

A grid convergence test was also completed for the structural model using the ASME standard to determine the suitability of the SOLID186

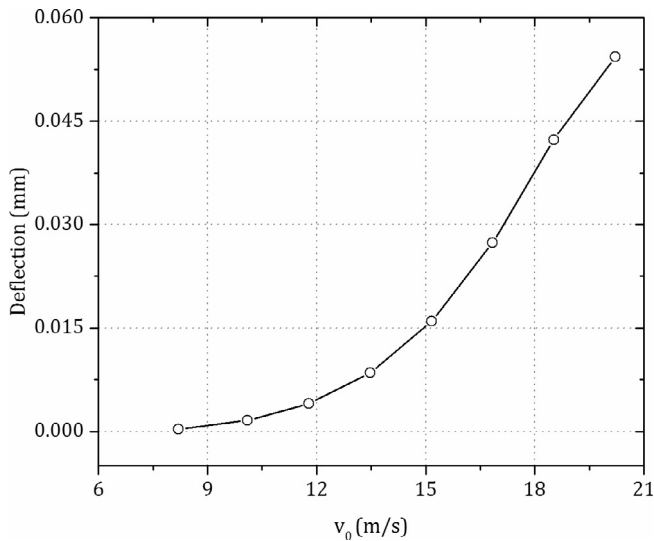


Fig. 8. Deflection of Plate 2 at 100 mm from the outlet end for different coolant velocities, with the support comb at the inlet end of the plates.

and CONTACT174 elements as well as the mesh. Although the GCI method was initially proposed for CFD and heat transfer calculations, it has also been recommended for finite element applications in structural and solid mechanics (Kwaśniewski, 2013).

Static analyses were performed using the Static Structural module of ANSYS Mechanical; a uniform pressure load ( $P$ ) of 135,444 Pa was applied over one of the long surfaces of each plate and the response of

the solid domain was calculated. This pressure loading was applied to simulate the hydraulic pressure load that the plates are exposed when coupled with the fluid domain. The other conditions of the plates and the support comb were preserved.

Table 4 shows the characteristic of the studied meshes. For this analysis, the deflection at the midpoint ( $\delta_m$ ) of the plates was chosen as the key parameter. Table 5 illustrates the uncertainty quantification of the structural model. It can be observed that the uncertainty from the finest mesh was 0.27%. Based on the results from the GCI analysis, a mesh with 299,656 hexahedral elements was used in the solid domain of the multiphysics model.

### 3.3. Validation study

In order to validate the FSI simulations for use in the analysis of fuel assemblies, a single plate test section designed by Kennedy (2015) was modeled. Kennedy conducted a set of experiments utilizing a flat plate, made from Aluminum Alloy 6061-T6, and located between two fluid channels with unequal thicknesses, 2.5420 mm and 2.032 mm, correspondingly. The wetted plate width ( $w$ ) is 110.287 mm, thickness ( $a$ ) is 1.016 mm, length plate ( $L_p$ ) is 647.7 mm, inlet plenum length ( $L_i$ ) is 190.5 mm and outlet plenum length ( $L_o$ ) is 76.2 mm. Along either side of the plate, a width of 12.7 mm was used for clamping it. The outer walls of the test section were constructed of Plexiglas panels. Fig. 4(a) depicts the longitudinal view of the experiment test section and Fig. 4(b) shows a transparent view of the FSI model. The materials properties are given in preceding sections.

To do the comparison, one case with an inlet flow rate of 2.6 kg/s was selected. A hexahedral mesh with 607,200 elements for the fluid domain and 108,120 elements for the solid domain was used. Most of

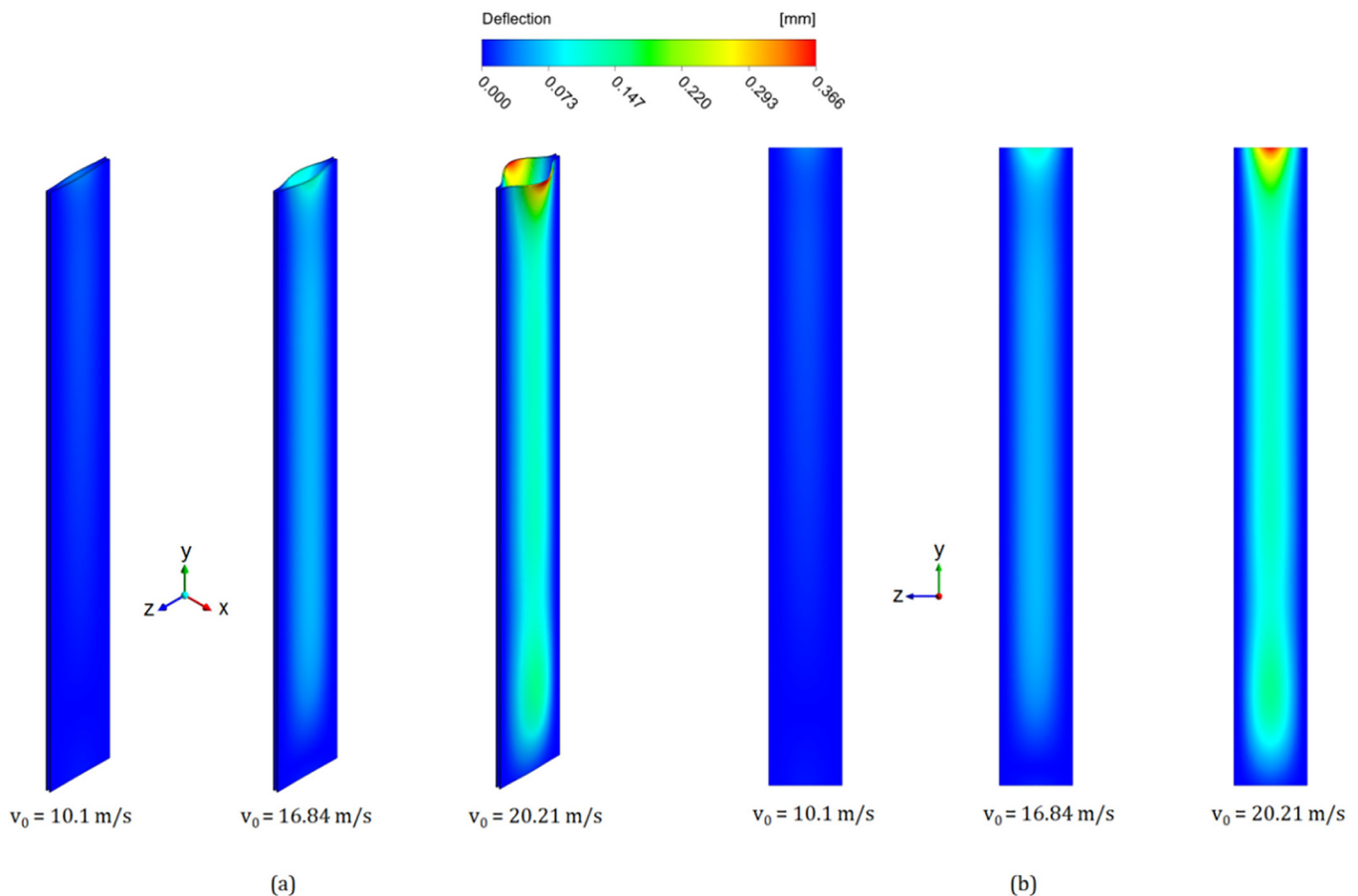


Fig. 9. Contours of deflection of the plates for different coolant velocities, without the support comb at the inlet end of the plates. (a) Isometric view and (b) frontal view. Flow moves in the  $-y$  direction. The deformation scale factor is  $0.5 \times$  [modified from (González Mantecón and Mattar Neto, 2018)].

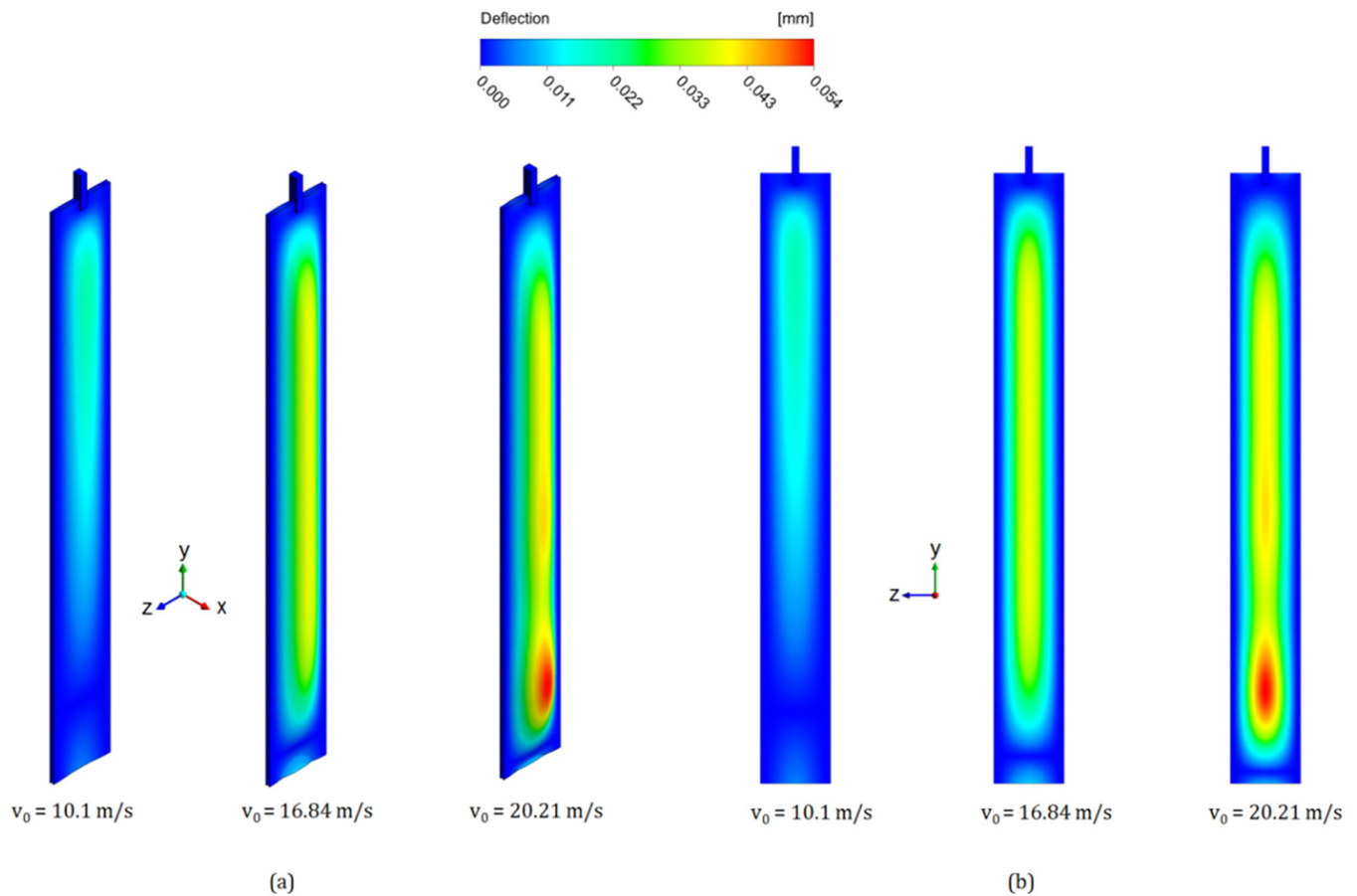


Fig. 10. Contours of deflection of the plates for different coolant velocities, with the support comb at the inlet end of the plates. (a) Isometric view and (b) frontal view. Flow moves in the  $-y$  direction. The deformation scale factor is  $0.5 \times$ .

the simulation conditions described in earlier sections were considered, with the difference that all the surfaces of this fluid domain were defined as no-slip smooth walls.

Kennedy provided average deflection points of the plate at different axial locations, measured with two laser displacement sensors. Fig. 5 presents the deflection comparison between the experimental results and the numerical model. In the figure, the error bars indicate the 95% confidence interval. As it can be seen, the leading and trailing edge deflections calculated with the FSI model showed a good agreement with the experiment. However, for the inner points, the deflection differ. This discrepancy is a result of imperfections on the plate surfaces, which were studied by Kennedy but not assumed in this FSI model. Nevertheless, the validation study allowed proof of the modeling approach and the capability of the computational tools to predict the plate deflections.

#### 4. Results and discussion

In the present work, prior to conducting the simulations, a set of target volumetric flow rates at the inlet was determined. Firstly, considering that 8.2 m/s is the minimum fluid velocity required in an RMB’s fuel element, using its nominal dimensions and an incompressible fluid, the smallest fluid flow rate was estimated. Afterward, new volume flow rates were calculated at velocity ratios  $v_0/v_M$  equal to 0.6, 0.7, 0.8, 0.9, 1.0, 1.1 and 1.2. The Miller’s critical velocity of the fuel element here analyzed is 16.84 m/s and was determined with Eq. (1), taking into account nominal dimensions and materials properties at room temperature. Table 6 provides those targeted values.

The first numerical experiment was performed and the structural

response was obtained. Next, this solution was taken as an initial condition and the new analyses were carried out. Every calculation was run until the convergence criterion was reached and steady-state solutions of the fluid flow and structure variables were achieved, e.g. pressure drop, the fluid force acting on the plates, and the total displacement of the midpoint of the plates. In all simulations, the dimensionless normal distance from the wall ( $y^+$ ) was checked to verify if the wall distance requirements for the  $k-\epsilon$  model were satisfied. It was found that  $30 < y^+ < 100$ ; for the near wall treatment, this is an appropriate range when the wall function approach is used (ANSYS Inc., 2017a). All runs were executed on an Intel Xeon E5-2640 workstation, 2.00 GHz, and 48 gigabytes of RAM.

Through each coolant channel and each plate, line probes were created along their axial centerline. From the coolant channels, static pressure profiles were extracted and the pressure differences between the central channel and the side channels were estimated. For both lateral channels, identical pressure profiles were observed. The resulting pressure differentials for all the flow rates are shown in Fig. 6(a). In the case of the plates, total mesh displacements were taken along the line probes. With these displacements, a static deflection profile of each fuel plate was built. Only deflection profiles of Plate 2 are shown in the following figures because similar profiles were detected for both plates. As can be seen in Fig. 6(b), with the increment of the fluid velocity, the resulting force on the plate and the plate deflections also increased. In addition, a region of incremented pressure difference and deflection began to appear near the trailing edge.

A comparison between the plate deflection profiles when the inlet support comb is used and when it is neglected is presented in Fig. 7. The case without the inlet support comb was previously studied and published in reference (González Mantecón and Mattar Neto, 2018). In that

study, the authors identified the occurrence of static deflections at the inlet and along the length of the plates, similar to what other papers anticipated. Additionally, it was also found that the critical velocity calculated with the numerical model coincided with the Miller's velocity.

From Fig. 7 can be concluded that, with the rise of the fluid velocity and without the support comb, the deflection at the inlet edge increased and a deflection peak appeared close to the outlet end. On the other hand, with the supporting comb, the static divergence at the leading edge of the plates is eliminated. However, it is interesting to note that even with the comb the plates are prone to deflect and the maximum deflection occurred near the trailing edge. It is noteworthy that a similar behavior was observed in an actual fuel assembly by Groninger and Kane (1963) and experimentally detected by Smitsaert (1968).

Fig. 8 depicts the variation of the plate deflection at 100 mm from the outlet end, without the support comb at the leading edge of the plates. It should be noted that the curve becomes increasingly more non-linear with an increase in flow rate. This fact indicates that there is still a significant deflection away from the inlet, which could restrict the flow passages and affect the safe operation of the reactor. During these runs, a point of instability was not identified as it was done in the previous work without the inlet comb (González Mantecón and Mattar Neto, 2018).

Deflection contours of the plates for the configurations without and with an inlet support comb are shown in Figs. 9 and 10, respectively. Comparing these contour plots, it can be noticed how the shape of the deformation changed and the effect of the comb limiting the leading edge deflection. The figures deserve the reader's attention because different scales are used. In all cases, the deflections were well within the elastic limit of the material.

## 5. Conclusions

In this paper, a numerical study of nuclear fuel plates with an inlet support comb was presented. The numerical setup was based on the two-way FSI technique in which the fluid flow loads determined by the CFD model are sent to the structural model as boundary conditions. Then, the displacements of the solid domain are transmitted back to the fluid dynamics analysis. The adopted model is representative of the fuel plates and coolant channels projected for the RMB reactor.

The numerical simulations predicted a behavior similar to that indicated in the literature. It was found that the static divergence at the inlet end was effectively eliminated with the installation of a support comb. Nevertheless, within the limits of the conditions considered herein, a significant deflection was identified near the outlet edge and it was an increasing function of the average velocity of the coolant in the channels. The results presented in this work show that, even with a support comb, the plates are prone to deflection along their length when the mass flow rate is raised. As a consequence, the flow channels could be constricted or completely closed, thus affecting the safe operation of the reactor. So, the authors consider that more studies, both experimental and numerical, should be done for an in-depth understanding of the advantages and limitations of the support comb.

## Acknowledgment

This study was financed by the Coordenação de Aperfeiçoamento de Pessoal de Nível Superior – Brasil (CAPES) – Finance Code 001.

## Appendix A. Supplementary data

Supplementary data to this article can be found online at <https://doi.org/10.1016/j.nucengdes.2018.12.009>.

## References

- Adams, T., Grant, C., Watson, H., 2012. A simple algorithm to relate measured surface roughness to equivalent sand-grain roughness. *Int. J. Mech. Eng. Mechatronics* 1.
- Andrade, D.A., de Angelo, G., Angelo, E., Di Giovanni Santos, P.H., Vaz, Branco, de Oliveira, F., Torres, W.M., Umbehaun, P.E., Batista De Souza, J.A., Belchior Junior, A., Sabundjian, G., de Carvalho Prado, A., 2015. A CFD Numerical Model for the Flow Distribution in a MTR Fuel Element. *Proceedings of the 2015 International Nuclear Atlantic Conference – INAC. Brazilian Nuclear Energy Association, São Paulo, Brazil.*
- ANSYS Inc., 2017a. ANSYS CFX Documentation – Release 18.2.
- ANSYS Inc., 2017b. ANSYS Mechanical Documentation – Release 18.2.
- ASM International, 1990. *ASM Handbook, Volume 2 Properties and Selection: Nonferrous Alloys and Special-Purpose Materials, 10th ed.* ASM International.
- ASME, 2009. *Standard for Verification and Validation in Computational Fluid Dynamics and Heat Transfer.* ASME V&V, pp. 20–2009.
- Fan, W., Peng, C., Guo, Y., 2015. CFD study on inlet flow blockage accidents in rectangular fuel assembly. *Nucl. Eng. Des.* 292, 177–186. <https://doi.org/10.1016/j.nucengdes.2015.06.016>.
- González Mantecón, J., Mattar Neto, M., 2018. Numerical methodology for fluid-structure interaction analysis of nuclear fuel plates under axial flow conditions. *Nucl. Eng. Des.* 333, 76–86. <https://doi.org/10.1016/j.nucengdes.2018.04.009>.
- Groninger, R.D., Kane, J.J., 1963. Flow induced deflections of parallel flat plates. *Nucl. Sci. Eng.* 16, 218–226. <https://doi.org/10.13182/NSE63-A26503>.
- Ho, M., Hong, G., Mack, A.N.F., 2004. *Experimental Investigation of Flow-Induced Vibration in a Parallel Plate Reactor Fuel Assembly.* Australia, Sydney.
- INVAP, 2013. *Brazilian Multipurpose Reactor Project – Core Thermal-Hydraulic Design in Forced Convection.* RMBP-0130-2HIN-005-A.
- Johansson, E.B., 1959. *Hydraulic Instability of Reactor Parallel-Plate Fuel Assemblies.* Knolls Atomic Power Laboratory, USA 10.2172/4221444.
- Kennedy, J.C., 2015. *Development and Experimental Benchmarking of Numeric Fluid Structure Interaction Models for Research Reactor Fuel Analysis* (PhD Dissertation). University of Missouri.
- Kwaśniewski, L., 2013. Application of grid convergence index in FE computation. *Bull. Polish Acad. Sci. Tech. Sci.* 61, 123–128. <https://doi.org/10.2478/bpasts-2013-0010>.
- Miller, D.R., 1958. Critical flow velocities for collapse of reactor parallel-plate fuel assemblies. *J. Eng. Power.* <https://doi.org/10.2172/4199355>.
- Perrotta, J.A., Soares, A.J., 2015. RMB: the new brazilian multipurpose research reactor. *Int. J. Nucl. Power* 60, 30–34.
- Rao, A., 2003. *Fluid-solid interaction analysis using ANSYS/multiphysics.* In: 2nd MIT Conference on Computational Fluid and Solid Mechanics 2003. Elsevier Science, Boston, USA, pp. 1492–1496.
- Smitsaert, G.E., 1968. Static and dynamic hydroelastic instabilities in MTR-type fuel elements Part I. Introduction and experimental investigation. *Nucl. Eng. Des.* 7, 535–546. [https://doi.org/10.1016/0029-5493\(68\)90103-9](https://doi.org/10.1016/0029-5493(68)90103-9).
- Smitsaert, G.E., 1969. Static and dynamic hydroelastic instabilities in MTR-type fuel elements part II. Theoretical investigation and discussion. *Nucl. Eng. Des.* 9, 105–122. [https://doi.org/10.1016/0029-5493\(69\)90052-1](https://doi.org/10.1016/0029-5493(69)90052-1).
- Stromquist, W.K., Sisman, O., 1948. *High Flux Reactor Fuel Assemblies Vibration and Water Flow.* Problem Assignment No. TX5-12. Oak Ridge National Laboratory, USA 10.2172/4351600.
- Tentner, A., Bojanowski, C., Feldman, E., Wilson, E., Solbrekken, G., Jesse, C., Kennedy, J., Rivers, J., Schnieders, G., 2017. Evaluation of Thin Plate Hydrodynamic Stability through a Combined Numerical Modeling and Experimental Effort. Argonne National Laboratory, USA ANL/RTR/TM-16/9.